

Article

Numerical Simulation and Analysis of Vibrating Rice Filling Based on EDEM Software

Hao Yuan *, Shifei Liang, Jing Wang and Yikang Lu

School of Mechanical Engineering, Jiangsu University, Zhenjiang 212000, China

* Correspondence: yuanhao@ujs.edu.cn

Abstract: An automatic rice-filling device for lotus root with glutinous rice was developed based on the process of artificial filling. In order to find the best parameters for the vibrating rice-filling device—feeding speed, filling height, funnel diameter, amplitude, and frequency—so as to reduce the time and improve the mass of rice filling, EDEM software (EDEM 2022) was used to conduct numerical simulation of the process and analyze the influence of various factors on the rice-filling time. The optimal combination of parameters for the highest quality of rice filling was determined as follows: rice feeding speed, 1.4 kg/s; height of rice filling, 30 mm; funnel diameter, 55 mm; amplitude, 0.6 mm; frequency, 50 Hz; and filling time, 3.4 s. The simulation experiment results are in good agreement with the prototype experiment, achieving the purpose of improving the efficiency of rice filling. This study provides theoretical guidance for research on an automatic rice-filling device for lotus root with glutinous rice.

Keywords: lotus root with glutinous rice; prototype experiment; theoretical analysis; optimal parameters; highest rice quality and production efficiency



Citation: Yuan, H.; Liang, S.; Wang, J.; Lu, Y. Numerical Simulation and Analysis of Vibrating Rice Filling Based on EDEM Software. *Agriculture* **2022**, *12*, 2013. <https://doi.org/10.3390/agriculture12122013>

Academic Editor: Ritaban Dutta

Received: 8 November 2022

Accepted: 24 November 2022

Published: 25 November 2022

Publisher's Note: MDPI stays neutral with regard to jurisdictional claims in published maps and institutional affiliations.



Copyright: © 2022 by the authors. Licensee MDPI, Basel, Switzerland. This article is an open access article distributed under the terms and conditions of the Creative Commons Attribution (CC BY) license (<https://creativecommons.org/licenses/by/4.0/>).

1. Introduction

Lotus root with glutinous rice and osmanthus is a special snack in the Jiangnan region of China. In recent years, because of its rich nutritional value and unique taste, it has become widely loved by consumers and its sales volume has grown rapidly. Its preparation is tedious. The traditional hand-made method is to soak glutinous rice and then pour it into cut lotus root with osmanthus sauce and brown sugar, and then cook it [1]. The production of lotus rice with glutinous rice in an industrial workshop mainly includes peeling, cutting, and capping the lotus root, filling it with rice, capping, and cooking. Among the steps, rice filling is the most tedious, and the manual method is still used [2,3]. The efficiency of rice filling greatly limits the efficiency of the whole production line of lotus root with glutinous rice. In order to improve the production efficiency, it is urgent to solve the problem of automatic rice filling. The purpose of the self-developed vibrating rice-filling device described in this paper is to solve the problem of a large amount of labor and low efficiency in manual rice filling. The time and mass of rice filling depend on several important parameters of the vibrating device, including the amplitude and frequency of the vibrating motor, the speed of hoist, the diameter of the rice-filling funnel, and the height of the rice filling.

At present, many scientific research institutes have studied the motion mechanism of particle flow in different situations, especially in crops, by the discrete element method. For example, in 2020, Jianfeng and others used EDEM software to analyze the maximum emission speed of different helical angles and the force acting on fertilizer or seed particles [4]. In 2016, Cunha et al. studied the repose angle of coniferous seed and soybean as a single particle and a binary mixture through discrete element numerical simulation and experimentation. Comparing the simulation results with the experimental values, they determined the best DEM parameter combination [5]. In 2021, Wenbo et al. simulated and

calibrated contact parameters of barley by EDEM software, and carried out verification tests to verify that the parameters were reliable [6]. In 2017, Dandan and others used EDEM-CFD software (EDEM 2022) to simulate and test an internal inflatable blown corn planter, optimize its structural parameters, and improve its working performance [7].

The discrete element method (DEM) for material analysis of discrete particle bodies was first proposed by Cundall, an American scholar, in 1971 based on the molecular dynamics principle. It was first applied to the analysis of rock mechanics problems [8,9]. The basic idea of the DEM is to separate discontinuity into a set of rigid elements so that each rigid element meets the kinematic equation. The kinematic equation of each rigid element is solved by the time-step iteration method, and then the overall motion form of the discontinuity is obtained. This method allows relative motion between units and does not necessarily satisfy the conditions of continuous displacement and deformation coordination, it has fast calculation speed and small storage space, and is particularly suitable for solving large displacement and nonlinear problems [10–12].

In this study, to determine the influence of different factors on the results of rice filling, the movement law of glutinous rice particles in a funnel and lotus root holes was studied by using the discrete element method. Through EDEM software, the process of vibrating rice filling was simulated and analyzed under conditions of different falling speeds, filling height, funnel diameter, amplitude, and frequency, and the effect of each parameter on filling time was obtained. Finally, the best combination of parameters was obtained by orthogonal test [13–15].

2. Materials and Methods

2.1. Structural Design and Working Principle of Vibrating Rice-Filling Device

According to the manual production of lotus root with glutinous rice and the production process of the workshop, the technical steps for automatic filling were as follows:

A 7-hole lotus root was selected, and a group was randomly selected from the lotus root samples provided by the company to meet the processing requirements. The shape and size of the lotus root were measured. Based on the process requirements provided by the company, the length and diameter of the lotus root were 160–210 mm and 60–85 mm, respectively.

On the thicker end of the lotus root, we cut off about 30–35 mm smoothly and left it as the cover; the rest was the segment for rice filling. In this way, the hole on the end face of the lotus root section can be as large as possible after removing the cover, which is conducive to improving rice-filling efficiency.

Each lotus section was filled with rice, and no gap segments had no rice.

To coordinate with the packing equipment for lotus root with glutinous rice, the filling efficiency needs to reach 2 s/piece.

The process achieved the recycling of rice and improved the corresponding utilization rate.

According to the current production situation of enterprises and the above technical steps, the overall structural design of the automatic rice-filling device was carried out, as shown in Figure 1. It mainly includes the glutinous rice hoist, the vibrating rice-filling mechanism, the fallen rice recycling mechanism, the lotus root with glutinous rice conveyance, and the automatic blanking mechanism. The glutinous rice hoist uses a spiral or scraper hoist, while the remaining mechanisms are designed independently.

Working principle: First, add enough washed glutinous rice to the rice bin of the hoist; the hoist lifts the rice to a certain height so that it falls into the vibrating filling mechanism. The vibrating rice-filling mechanism includes 5 stations that can fill the lotus root simultaneously. The function of the fallen rice recycling mechanism is to recover the rice grains that do not fill in the lotus root sections into the bin of the glutinous rice hoist. The conveyor chain circulation mode is adopted for feeding the glutinous rice into the lotus root to achieve continuous work and ensure the filling speed. The automatic feeding mechanism can transfer the filled lotus root from the transport chain to the subsequent packaging equipment.

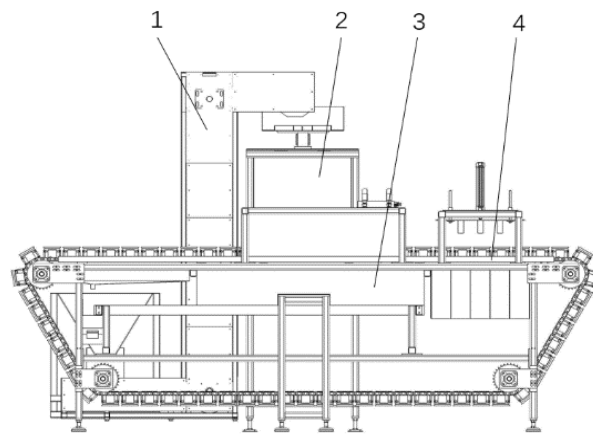


Figure 1. Diagram of overall structure of automatic filling device for lotus root with glutinous rice. 1. Glutinous rice hoist; 2. vibrating rice-filling mechanism; 3. fallen rice recycling mechanism; 4. lotus root with glutinous rice conveyance and automatic blanking mechanism.

To ensure the mass, shorten the time, and improve the efficiency of rice filling, the process of vibrating rice filling needed to be simulated and analyzed. First, the model of the vibrating rice-filling mechanism was simplified. To improve the simulation efficiency, only the parts which directly contact the glutinous rice particles were separated. The simplified model is shown in Figure 2.

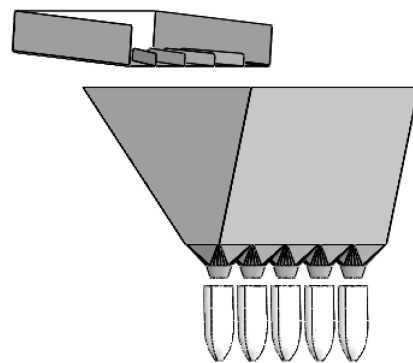


Figure 2. Model simplification of vibrating rice-filling mechanism.

The lotus root segment model after removing the cap was established with the maximum sample size. The length was 180 mm, the diameter was 75 mm, and the center distance to the central lotus root hole was 40 mm.

2.2. EDEM Software

EDEM is the first multi-purpose discrete element method modeling software in the world; it can be used for simulation and analysis of particle treatment and production processes of industrial manufacturing equipment. Users can easily and quickly create parametric models of particle entities using EDEM. To reflect the shape of actual particles, users can import CAD entity models directly into EDEM, which will greatly increase the accuracy of simulation. In addition, forces, material properties, and other physical properties can be added to EDEM to form particle models, which can be stored in the software database; this can enable users to build personalized model processing environments.

2.3. Establishment of Rice-Filling Contact Model

The essence of the rice-filling process is to transfer energy through contact and collision between particles and funnels, particles and lotus roots, and particles and particles, and finally achieve the purpose of moving the particles and filling the lotus roots. Because

the glutinous rice consists of wet particles after cleaning, the Hertz–Mindlin model with the JKR model is used for the collision process between particles and the geometry, and between the particles [16–19], as shown in Figure 3.

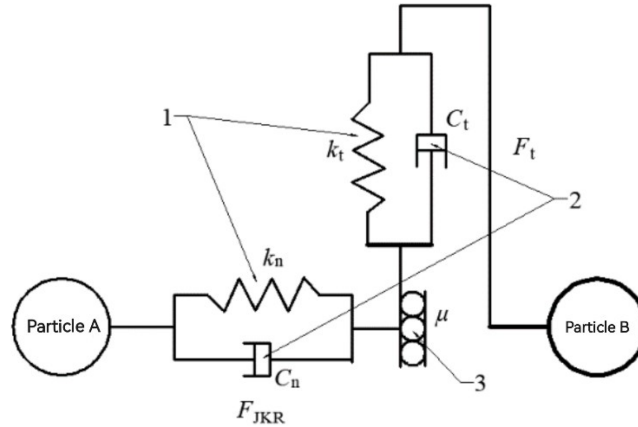


Figure 3. Contact mechanical model: 1. particle stiffness (spring); 2. damper; 3. friction. F_{JKR} is the normal force of JKR model, F_t is tangential force, k_n is normal stiffness, k_t is tangential stiffness, C_n is the normal damping coefficient, C_t is the tangential damping coefficient, μ is the coefficient of friction.

Through contact mechanics analysis, we can get:

$$F_n^d = -2\sqrt{\frac{5}{6}}\beta\sqrt{S_n m^* v_n^{rel}} \tag{1}$$

$$F_t = -S_t \delta \tag{2}$$

$$F_t^d = -2\sqrt{\frac{5}{6}}\beta\sqrt{S_t m^* v_t^{rel}} \tag{3}$$

The Hertz–Mindlin with JKR model is consistent with the Hertz–Mindlin (no slip) model in terms of calculating normal damping force, tangential elastic force, and tangential damping force. However, the normal elastic force of the JKR model depends on the overlap between particles, particle surface energy, and interaction parameters. The specific calculation formula is as follows [20]:

$$F_{JKR} = -4\sqrt{\pi \cdot \gamma \cdot E^*} a^{\frac{3}{2}} + \frac{4E^*}{3R^*} a^3 \tag{4}$$

where F_n^d is normal damping force (N); F_t is tangential elastic force (N); F_t^d is tangential damping force (N); F_{JKR} is the normal elastic force in the JKR model (N); R^* is the equivalent particle radius (m); E^* is the equivalent elastic modulus (Pa); α is the normal overlap between particles (m); m^* is the equivalent mass (kg); v_n^{rel} is normal relative velocity (m/s); v_t^{rel} is tangential relative velocity (m/s); γ is particle surface energy (J/m²); and a is contact radius of two particles (m).

S_n , β , and S_t can be calculated by:

$$S_n = 2E^* \sqrt{R^* \alpha}$$

$$\beta = \frac{\ln e}{\sqrt{\ln^2 e + \pi^2}}$$

$$S_t = 8G^* \sqrt{R^* \alpha}$$

where e is the coefficient of restitution and G^* is the equivalent shear modulus (MPa).

2.4. Calibration of Simulation Parameters

In discrete element simulation, the selection of the contact model, the material characteristic parameters and geometry of particles, and the mutual contact parameters have a crucial impact on the authenticity and accuracy of the simulation results. Material characteristic and contact parameters can be calibrated by consulting the literature, testing, or using virtual experiments according to the simulation requirements. The material characteristic and contact parameters required in this paper were determined by accumulation and kinematics tests [21].

The required material property parameters of glutinous rice, 304 stainless steel, and lotus root are shown in Table 1 [22,23].

Table 1. Mechanical properties of materials.

Material	Poisson Ratio	Shear Modulus (MPa)	Density (g/cm ³)
Glutinous rice	0.3	2.6	1.35
SUS304	0.285	7.9×10^4	7.93
Lotus root	0.35	1.3	1.20

The contact parameters were divided into particle-to-particle and particle-to-geometry parameters, mainly including static friction coefficient, rolling friction coefficient, and collision recovery coefficient. The parameters are shown in Table 2 [24–26].

Table 2. Contact parameters between materials.

Interaction	Restitution Coefficient	Static Friction Coefficient	Rolling Friction Coefficient
Glutinous rice–glutinous rice	0.3	0.5	0.01
Glutinous rice–SUS304	0.5	0.3	0.01
Glutinous rice–lotus root	0.1	0.8	0.1

For the calibration of surface energy between glutinous rice particles by an accumulation angle experiment [27], a series of corresponding stacking angle values were obtained by modifying the surface energy parameter values for multiple simulation experiments. Then, the approximate parameters of surface energy between particles could be obtained by comparing them with the measured particle accumulation angle. The surface energy obtained by the stacking angle experiment was about 0.945 J/m².

In EDEM software, the simulation time step is set by the Rayleigh time step [28], and the size is generally set to 20 to 40% of the Rayleigh time step. The Rayleigh time step calculation method is as follows:

$$T_R = \frac{\pi R \left(\frac{\rho}{G}\right)^{\frac{1}{2}}}{(0.1631\nu + 0.8766)} \quad (5)$$

where R is the radius of the nanocrystal (m); ρ is the density (kg/m³); G is the shear modulus (MPa); and ν is the Poisson ratio.

EDEM software will automatically calculate the Rayleigh time step, and 0.2 T_R was selected as the time step. A group of 5 lotus roots was used for rice filling. We modified the values of influencing factors to carry out multiple simulations, used the data output function of the EDEM software's post-processing module to output the change trend of rice quality in lotus root sections with time, and processed the data with Origin software (version 9.0) to get the change curve of rice quality with time. Figure 4 shows the vibrating rice filling simulation.

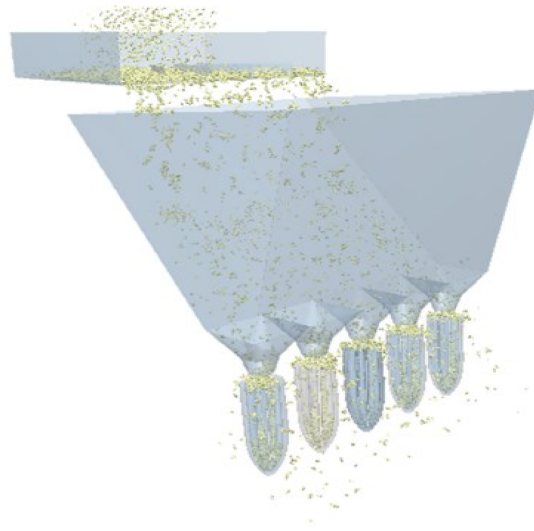


Figure 4. Simulation process of vibrating rice filling.

2.5. Prototype Test

In this paper, a prototype of a high-efficiency automatic rice-filling device for lotus root with glutinous rice was used for trial production. As shown in Figure 5, the prototype included a glutinous rice hoist, a vibrating rice-filling mechanism, a fallen rice recycling mechanism, a filled lotus root conveying mechanism, and an automatic blanking mechanism.



Figure 5. Prototype of automatic rice-filling device for lotus root with glutinous rice.

Lotus root samples for experimental glutinous rice production were provided by a lotus root food company. The samples were cut at the thickest part of the lotus root, and the total length and diameter of the lotus root were recorded, as shown in Table 3. The sample numbers of lotus root segments and covers are shown in Figure 6. The prototype experiment was carried out with the best group of influencing factors obtained by simulation.

Table 3. Size of lotus root sections.

Number	Total Length of Lotus Root (mm)	Length of Rice-Filled Lotus Root Section (mm)	Maximum Diameter of Lotus Root (mm)
1	170	140	72
2	205	175	70
3	177	145	78
4	208	178	73
5	212	175	66
6	176	144	75
7	172	141	71
8	186	152	77
9	178	147	72
10	191	160	72
11	179	169	71
12	170	140	72
13	208	176	66
14	187	161	73
15	193	162	74
16	177	145	78
17	210	178	74
18	171	140	68
19	178	146	74
20	175	146	71
21	184	152	73
22	194	161	76
23	181	148	76
24	176	145	69
25	192	160	75

**Figure 6.** Lotus root sample number grouping.

2.6. Statistics and Analysis of Experimental Data

The data output function of the EDEM software post-processing module was used to output the change trend of waxy rice quality in lotus root sections with time. The data were processed by Origin software and the change curve of rice quality with time was obtained.

An orthogonal experiment was designed, and the results of the experiment were statistically analyzed using the SPSS software (version 9.0). Analysis methods include range analysis, variance analysis, and factor index analysis.

3. Results

3.1. Simulation Results and Analysis

3.1.1. Effect of Rice-Feeding Speed on Rice-Filling Time

When the funnel diameter d was 40 mm, the section height h of the rice-filling funnel and lotus root section was 20 mm, the amplitude A was 1 mm, and the frequency f of the vibration motor under the lotus root was 50 Hz; the simulation was performed with four feeding speeds: v_1 – $v_4 = 0.5, 0.75, 1.0,$ and 1.25 kg/s, respectively. The specific parameters are shown in Table 4.

Table 4. Simulation parameters at different rice-feeding speeds.

v (kg/s)	d (mm)	h (mm)	A (mm)	f (Hz)
$v_1 = 0.50$	40	20	1	50
$v_2 = 0.75$				
$v_3 = 1.00$				
$v_4 = 1.25$				

As shown in Figure 7, with an increased feeding speed v , the convergence rate of the mass curve grows faster, but the convergence rate of the adjacent two curves is lower. This shows that, with an increased rice-feeding speed, the filling speed increases gradually, but the improvement rate of rice-filling speed diminishes.

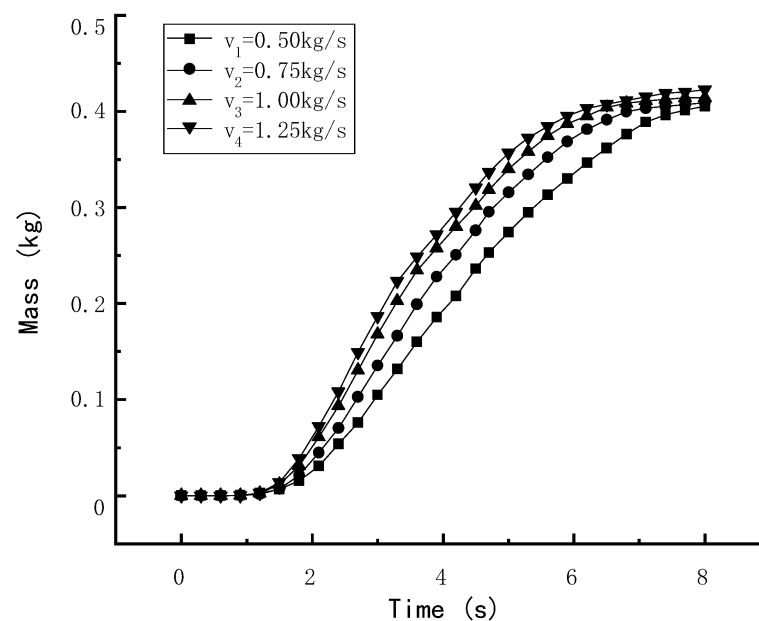


Figure 7. Curves of quality change of rice filling at different feeding speeds.

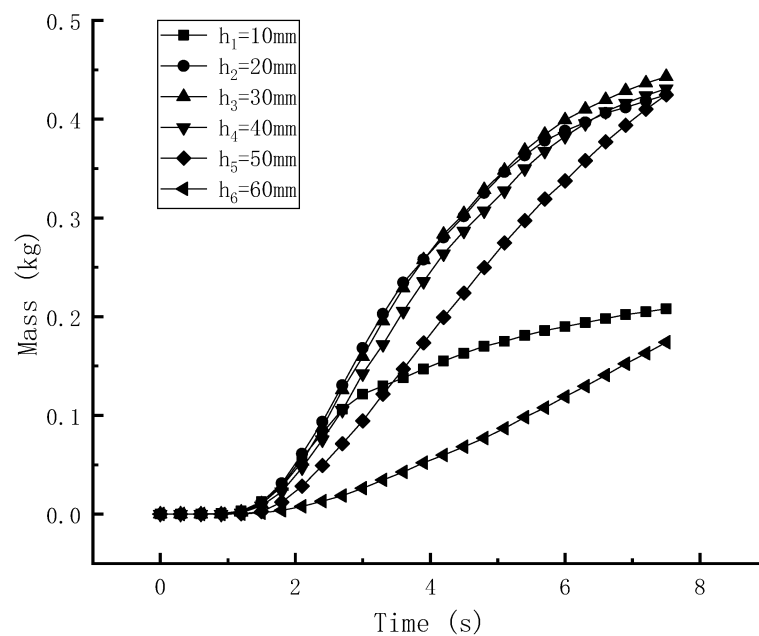
3.1.2. Effect of Filling Height on Filling Time

The setting of rice-feeding speed v refers to the analysis of its influence on rice-filling time in the previous section, and $v = 1.0$ kg/s is selected. Other parameters were set as follows: diameter of rice-filling funnel $d = 40$ mm, amplitude of vibration motor under lotus root $A = 1$ mm, and vibration frequency $f = 50$ Hz. The simulation was carried out with six filling heights: h_1 – h_6 : 10, 20, 30, 40, 50, and 60 mm. The specific parameter settings are shown in Table 5.

Table 5. Simulation parameters at different filling heights.

h (mm)	v (kg/s)	d (mm)	A (mm)	f (Hz)
$h_1 = 10$	1.0	40	1	50
$h_2 = 20$				
$h_3 = 30$				
$h_4 = 40$				
$h_5 = 50$				
$h_6 = 60$				

As shown in Figure 8, first, it can be seen that the lotus root could not be filled in 8 s when the rice-filling height was 10 mm (h_1) and 60 mm (h_6), whereas in the other four groups of simulations the lotus root was filled within 8 s. Among them, group h_5 at 50 mm had the slowest rice-filling speed compared with the other groups, and there was a large difference in rice-filling speed. The curves of the other three groups are very close, and the difference is not obvious. Among them, the fastest rice-filling speed was at 20 mm (h_2) and 30 mm (h_3). The curves of h_2 and h_3 are very close and intersect at $t = 3.9$ s. When $t < 3.9$ s, the rice-filling speed of h_2 was greater than that of h_3 . When $3.9 < t < 8$ s, the rice-filling speed of h_3 exceeded that of h_2 , and the curve converges first, indicating that the whole lotus root was filled.

**Figure 8.** Change curves of rice-filling quality with different heights of rice filling.

3.1.3. Effect of Funnel Diameter on Rice-Filling Time

The specific parameter settings of a simulation with rice-feeding speed $v = 1.0$ kg/s, height of rice filling $h = 20$ mm, funnel diameter $A = 1$ mm, and vibration frequency $f = 50$ Hz using funnel diameters d_1 – $d_5 = 20, 30, 40, 50,$ and 60 mm are shown in Table 6.

Table 6. Simulation parameters for different funnel diameters.

d (mm)	v (kg/s)	h (mm)	A (mm)	f (Hz)
$d_1 = 20$	1.0	20	1	50
$d_2 = 30$				
$d_3 = 40$				
$d_4 = 50$				
$d_5 = 60$				

As shown in Figure 9, when $d_1 = 20$ mm, the end face of the lotus root and funnel were blocked at $t = 2.5$ s. The convergence rates of the curves of the other four groups are similar, and the mass curve converges fastest when $d_4 = 50$ mm, indicating that the rice-filling speed is the fastest, which is more obvious in the first half stage. The curve convergence speed is the slowest when $d_2 = 30$ mm, and that of $d_3 = 40$ mm and $d_5 = 60$ mm is very close, indicating that the rice-filling speed of the two groups is similar.

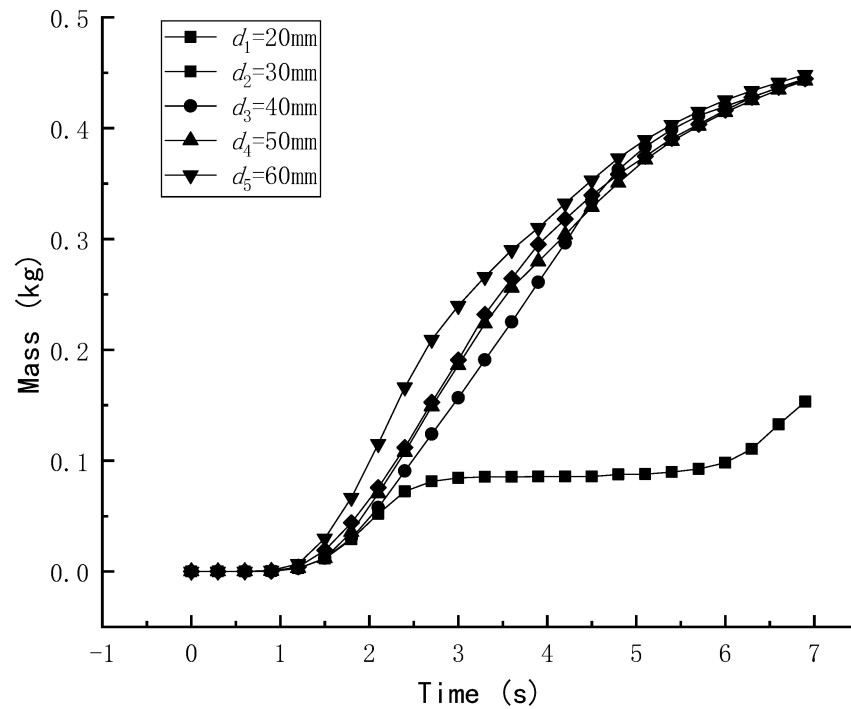


Figure 9. Variation curve of rice-filling mass with different funnel diameters.

3.1.4. Effect of Amplitude on Rice-Filling Time

The specific parameter settings of a simulation with rice-feeding speed $v = 1.0$ kg/s, height of rice filling $h = 20$ mm, funnel diameter $d = 50$ mm, and vibration frequency $f = 50$ Hz using A_1 – $A_5 = 0, 0.5, 1.0, 1.5,$ and 2.0 mm are shown in Table 7.

Table 7. Simulation parameters at different amplitudes.

A (mm)	v (kg/s)	h (mm)	d (mm)	f (Hz)
$A_1 = 0$				
$A_2 = 0.5$				
$A_3 = 1.0$	1.0	20	50	50
$A_4 = 1.5$				
$A_5 = 2.0$				

When $A_1 = 0$ mm, that is, no vibration is added below the lotus root, the rice was blocked at $t = 3.0$ s. Among the curves for other four groups, when $A_2 = 0.5$ mm, the curve convergence speed is the fastest and the rice-filling time is the shortest. With increased amplitude, it can be found that the simulation time of the four groups gradually increases; when $A_2 = 0.5$ mm, the rice-filling time is the shortest, and when $A_5 = 2.0$ mm, the rice-filling time is the longest. In addition, it can be found that, with increased amplitude, the increasing time of the four rice-filling simulation groups gradually decreases. From Figure 10, it can be seen that the convergence speed of $A_4 = 1.5$ mm and $A_5 = 2.0$ mm is almost the same.

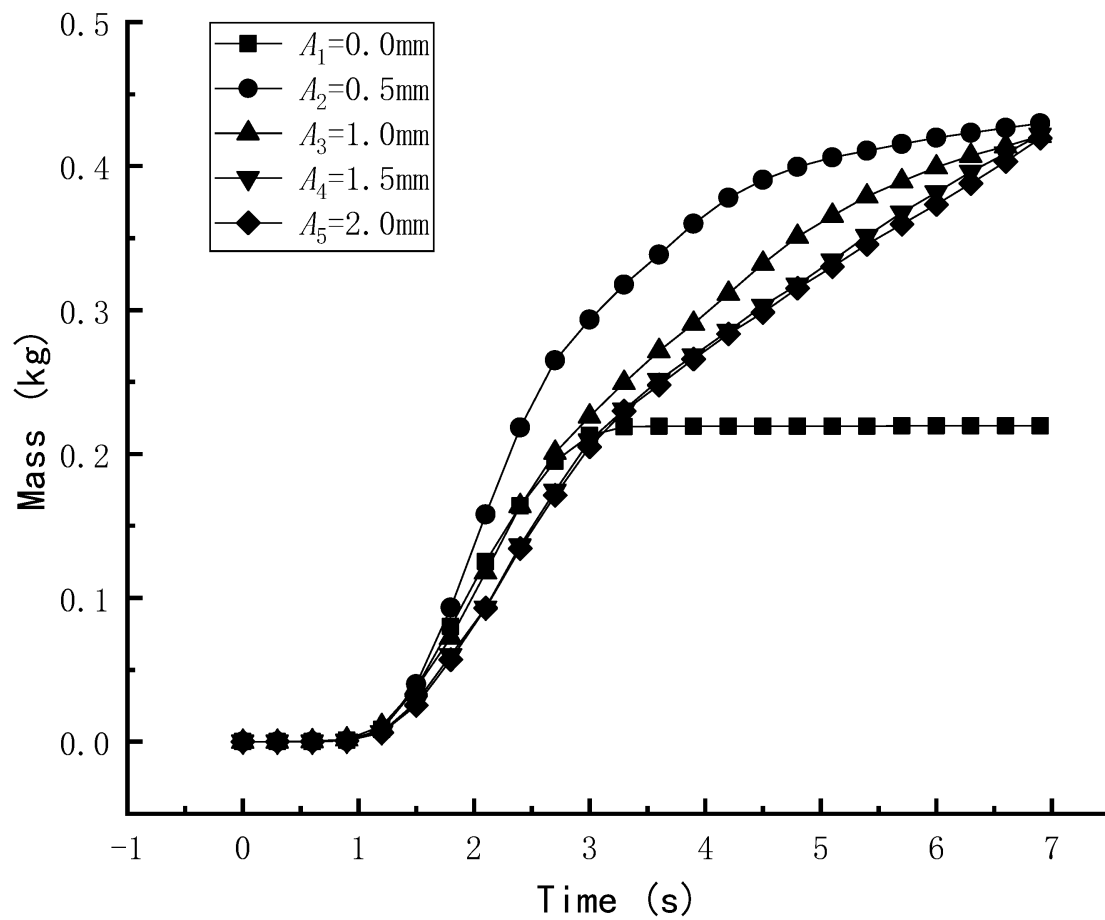


Figure 10. Variation curve of rice-filling mass with different amplitudes.

3.1.5. Effect of Frequency on Rice-Filling Time

The specific parameter settings of a simulation with rice-feeding speed $v = 1.0$ kg/s, height of rice filling $h = 20$ mm, funnel diameter $d = 50$ mm, and vibration frequency $A = 0.5$ mm using f_1 – $f_5 = 20, 30, 40, 50,$ and 60 Hz are shown in Table 8.

Table 8. Simulation parameters at different amplitudes.

f (Hz)	v (kg/s)	h (mm)	d (mm)	A (mm)
$f_1 = 20$	1.0	20	50	0.5
$f_2 = 30$				
$f_3 = 40$				
$f_4 = 50$				
$f_5 = 60$				

As shown in Figure 11, in the simulation using f_1 – $f_3 = 20, 30,$ and 40 Hz, with increased motor vibration frequency, the mass of glutinous rice increased at the same time. The simulation results show that the two groups $f_1 = 20$ Hz and $f_2 = 30$ Hz were not filled, and the group $f_3 = 40$ Hz met the requirements of filling lotus root. The curve shows that the convergence rate is slightly faster than that of $f_4 = 50$ Hz and $f_5 = 60$ Hz, but the final filling mass of $f_3 = 40$ Hz was slightly lower than that of $f_4 = 50$ Hz and $f_5 = 60$ Hz.

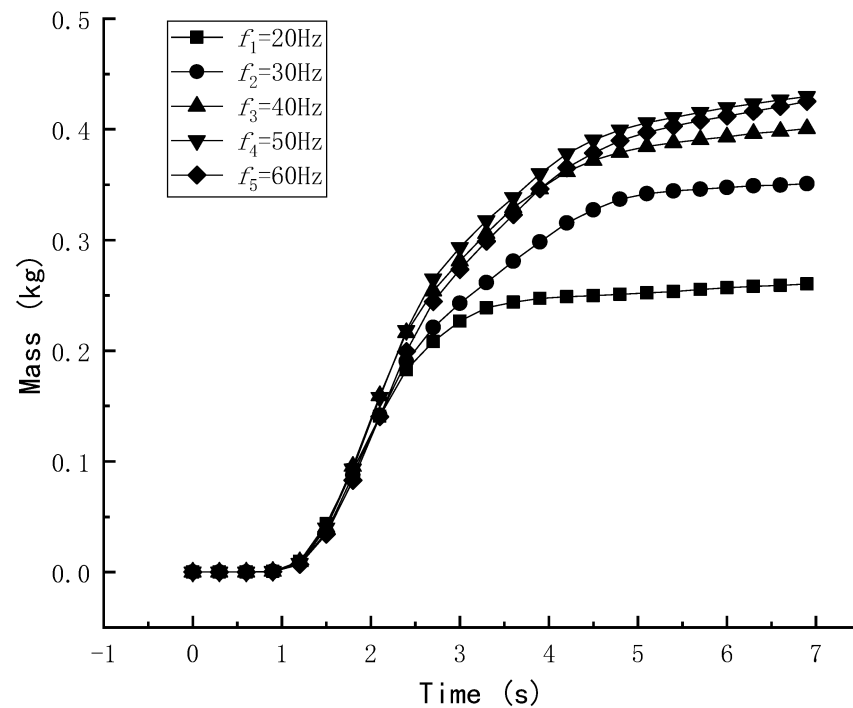


Figure 11. Curves of mass change of rice under different frequencies.

3.2. Determining the Best Combination of Factors

In the previous section, the effect of each factor on the filling time was analyzed by the control variable method to determine which factor was the main influencing factor, and we further determined the optimum parameter range of each influencing factor and refined the values near the optimum. The further values of feeding speed, filling height, funnel diameter, amplitude, and frequency are shown in Table 9.

Table 9. Secondary values of each parameter.

v (kg/s)	h (mm)	d (mm)	A (mm)	f (Hz)
0.8	20	40	0.2	40
1.0	25	45	0.4	45
1.2	30	50	0.6	50
1.4	35	55	0.8	55
1.6	40	60	1.0	60

Five levels were selected for each of the five factors. To simulate all possible combinations, $5^5 = 3125$ simulations would be required, which is not practical. Therefore, an orthogonal test can be used for grouping. An orthogonal test is a scientific method for selecting suitable and representative points among a large number of experimental points and arranging the experiments reasonably by using an orthogonal table, derived from Galois' theory [29,30].

The required orthogonal table in this paper is L25 (5^6). As shown in Table 10, only 25 simulations are needed, which saves much time. The orthogonal experimental results were analyzed and calculated using the SPSS software.

Table 10. Orthogonal experiment grouping.

Simulation Group	v (kg/s)	h (mm)	d (mm)	A (mm)	f (Hz)	t (s)
1	0.8	20	40	0.2	40	7.13
2	0.8	25	45	0.4	45	6.05
3	0.8	30	50	0.6	50	5.45
4	0.8	35	55	0.8	55	6.30
5	0.8	40	60	1.0	60	8.35
6	1.0	20	45	0.6	55	5.80
7	1.0	25	50	0.8	60	6.35
8	1.0	30	55	1.0	40	5.95
9	1.0	35	60	0.2	45	8.70
10	1.0	40	40	0.4	50	5.35
11	1.2	20	50	1.0	45	6.45
12	1.2	25	55	0.2	50	6.30
13	1.2	30	60	0.4	55	6.15
14	1.2	35	40	0.6	60	5.75
15	1.2	40	45	0.8	40	5.65
16	1.4	20	55	0.4	60	5.35
17	1.4	25	60	0.6	40	5.70
18	1.4	30	40	0.8	45	5.95
19	1.4	35	45	1.0	50	6.15
20	1.4	40	50	0.2	55	6.20
21	1.6	20	60	0.8	50	6.25
22	1.6	25	40	1.0	55	6.15
23	1.6	30	45	0.2	60	5.85
24	1.6	35	50	0.4	40	5.70
25	1.6	40	55	0.6	45	5.55
k_1	6.54	5.96	5.80	6.76	5.75	
k_2	6.43	6.11	5.90	5.72	6.54	
k_3	6.06	5.87	6.03	5.65	5.90	
k_4	5.87	6.52	5.89	6.10	6.12	
k_5	5.90	6.22	7.03	6.61	6.33	
R	0.67	0.65	1.23	1.11	0.79	

Independent variables: falling velocity v , filling height h , funnel diameter d , amplitude f , frequency A ; dependent variable: filling time t . K_i is the test index corresponding to the factor at level i ; R is extreme.

With the SPSS software, the primary and secondary effects of each factor were analyzed by range analysis; the larger the R-value in Table 10, the greater the impact on the experimental results. The results show that, within a certain range, five parameters have an influence on the filling time: funnel diameter, amplitude, frequency, speed, and height.

Significance level variance analysis (ANOVA) was performed using SPSS software to determine the effects of these five factors on the filling time [31]. Table 11 shows the results.

Table 11. Analysis of variance for orthogonal experiments.

Source	Type III Sum of Squares	df	Mean Square	F	Sig.
Corrected model	15.017 ^a	20	0.751	39.55	0.0095
intercept	955.181	1	955.181	5031.611	0.0000
v	2.418	4	0.605	13.185	0.0144
h	1.089	4	0.272	7.434	0.0368
d	4.632	4	1.158	16.100	0.0054
f	1.254	4	0.313	7.651	0.0320
A	5.624	4	1.406	27.407	0.0039
Error	0.759	4	0.190		
Total	970.957	25			
Corrected total	15.776	24			

^a. R Squared = 0.952 (Adjusted R Squared = 0.911).

The results in Table 11 show that the amplitude A and funnel diameter d have significant effects on the experimental results, the filling speed v has minor significant effects, and the vibration frequency f and filling height h have smaller effects.

Factor index analysis was carried out by SPSS software, and an effect fold chart of each factor was generated, as shown in Figure 12.

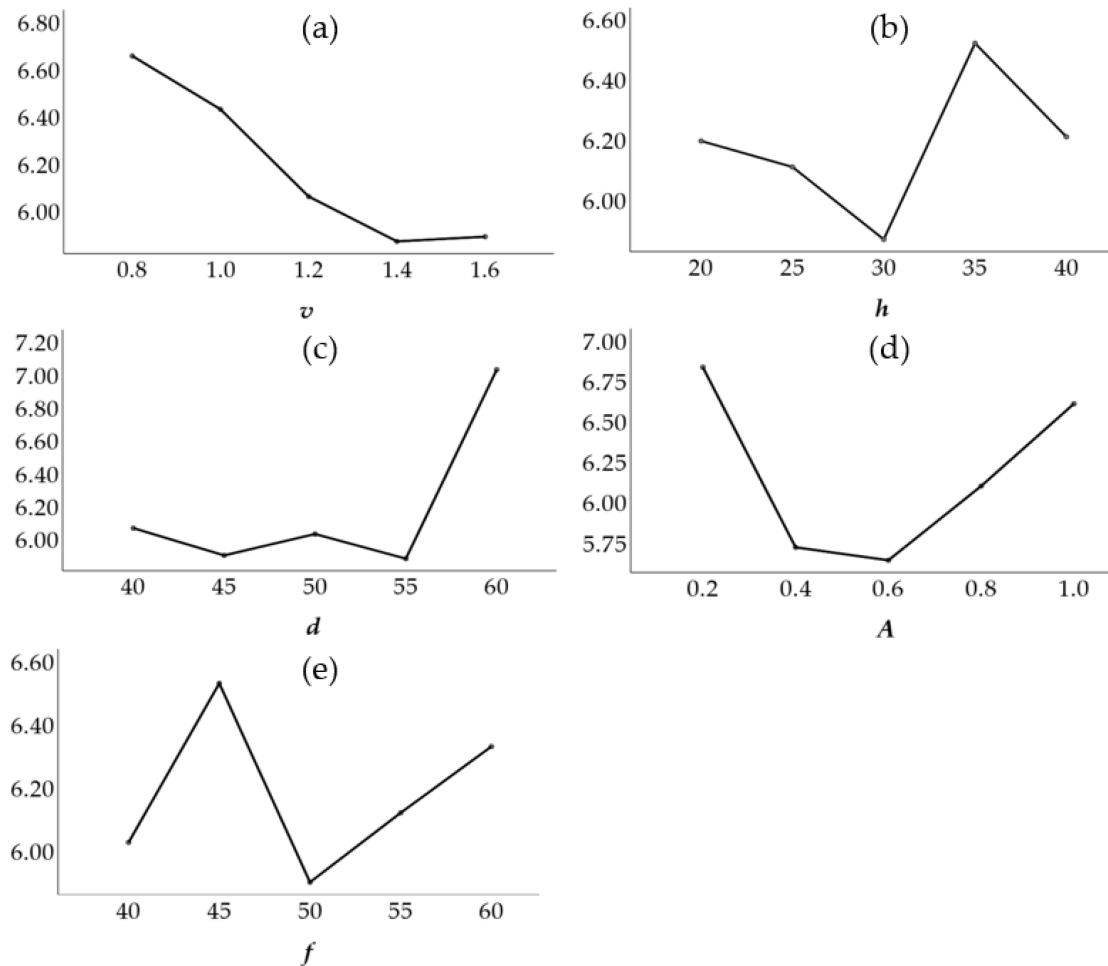


Figure 12. Fold chart of effects for each factor: (a) v , (b) h , (c) d , (d) A , (e) f .

Figure 12 shows that the optimum combination of parameters is $v = 1.4$ kg/s, $h = 30$ mm, $d = 55$ mm, $A = 0.6$ mm, and $f = 50$ Hz. Another simulation was carried out with this combination of parameters, and filling time $t = 3.4$ s was obtained.

In conclusion, the optimum combination of parameters is $v = 1.4$ kg/s, $h = 30$ mm, $d = 55$ mm, $A = 0.6$ mm, and $f = 50$ Hz for a filling time of $t = 3.4$ s. In a certain range, five parameters have an influence on filling time: funnel diameter, amplitude, frequency, feeding speed, and filling height.

3.3. Prototype Test Results

Prototype experiments were carried out with parameter values of $v = 1.4$ kg/s, $h = 30$ mm, $d = 55$ mm, $A = 0.6$ mm, and $f = 50$ Hz, and the rice-filling time was 3.4 s. The results of rice filling, shown in Figure 13, meet the production process requirements for lotus root with glutinous rice. Compared with manual rice filling, the efficiency is greatly improved.



Figure 13. Rice filling.

4. Discussion

In the simulation analysis of five single factor effects (Section 3.1), the rice-filling efficiency increased with increasing rice-loading speed within a certain range, but the increase diminished, causing congestion when it exceeded a certain upper limit. If the height of filling rice is too low, blockage will occur. If the height of filling rice is too high, the particles will diffuse outward and the filling time will be too long. However, within a certain range, there is little influence on the efficiency of filling rice. When the diameter of the funnel is too small, it will cause serious blockage of the funnel mouth. When the diameter of the funnel is close to the center distance of the lotus root hole, the filling effect is better, especially when the funnel diameter is 5 mm larger than that of the lotus root hole, and the influence on filling efficiency is obvious. Blockage will occur if vibration is not added or the amplitude is too small. In a certain range, with increased amplitude, the filling time increases, but the increase diminishes, indicating that the influence of amplitude on filling time decreases gradually, and the most obvious impact on filling efficiency is within an amplitude range of 0.5–1.0 mm. With increased frequency, the quality of rice filling increases continuously, and the gap in the lotus root hole goes from unsatisfactory to fully filled. The optimum frequency is 40–60 Hz, but the improvement is not obvious in this range.

In the above results of the simulation analysis of the influence of five single factors and the subsequent orthogonal simulation test (Section 3.2), the five parameters that mainly affected the filling time were funnel diameter, amplitude, frequency, speed, and height. Amplitude A and funnel diameter d had significant effects on the experimental results, while filling speed v had minor significant effects. Vibration frequency f and filling height h had certain effects on the experimental results, which are in agreement with the simulation. This further proves the correctness and feasibility of the test and analysis results.

In this study, the optimal combination of parameters for vibrating rice filling was obtained through numerical simulation and orthogonal tests. The simulation results were basically consistent with the experimental test results (Section 3.3), which realized the purpose of improving rice-filling efficiency, and also showed the correctness and feasibility of numerical simulation using EDEM software. The feasibility of simulation with EDEM software and the research method of orthogonal test analysis can also be verified in other existing studies. For example, in 2022, Jun and others used EDEM software to simulate the speed of a threshing drum and the angle of the guide plate in research on a rape threshing device. The validity of simulation analysis was further verified by three-factor and three-level orthogonal experiments [32]. In 2022, Yuyao et al. calibrated the parameters in a study on a soil discrete element model of potato tuber by discrete element simulation, and carried out a three-factor response surface test to prove that the calibration results were reliable [33].

With regard to research on automatic rice-filling devices at home and abroad, in 2010, Nie Xintian et al. put forward a kind of lotus root glutinous rice-filling machine that clamps

lotus root joints with different diameters by a cylinder installed with a silicone airbag and vibrates the rice-filling part by compound movement in the horizontal and vertical directions, so as to improve the rice-filling effect [34]. In 2018, Yan Shoulei et al. put forward an automatic filling device and a filling system for lotus root with waxy rice. They used a spring vibration device to fill multiple lotus roots with rice at the same time, which realized automatic filling in batches to a certain extent and improved the filling efficiency [35]. In 2019, Zhang Hong and others put forward an automatic rice-filling machine for lotus root that uses a rice-feeding module to ensure that the waxy rice particles are fully filled into the lotus root holes. A vibrating module applies vibration to the lotus root while clamping and fixing lotus roots with different diameters to improve rice-filling efficiency [36]. All of the above, and some other studies [37–39], applied vibration to lotus root and paid attention to controlling the rice-dropping speed and making the rice drop evenly, but did not further explore the rice-dropping speed, amplitude, and frequency, or the pressure in the filling equipment. The interaction of these factors will cause problems, such as the blockage of glutinous rice granules or the inability to fill lotus root holes during the rice-filling process, which will affect the final result.

This study examined the main factors affecting the results of rice filling, analyzed the effects of each factor on the results and their significance, and obtained the best combination of parameters, which provides certain value for related studies.

5. Conclusions

Based on the idea of DEM, EDEM software was used to carry out numerical simulation analysis of vibrating rice filling, and simulations of each influencing factor and the orthogonal test. The results of the simulation test were analyzed based on the data. The best combination of the five factors was $v = 1.2$ kg/s, $h = 25$ mm, $d = 45$ mm, $A = 0.8$ mm, and $f = 50$ Hz, the best rice filling time was 3.4 s, and the work efficiency met the production requirements. In a certain range, five parameters have an influence on filling time: funnel diameter, amplitude, frequency, top speed, and filling height. Optimizing these parameters significantly improves the efficiency of automatic vibrating rice-filling equipment. The simulation results are basically in agreement with the results of prototype experiments, which confirms the feasibility of numerical simulation analysis using the EDEM software.

Author Contributions: Conceptualization, H.Y. and S.L.; Methodology, Y.L.; Investigation, J.W.; Resources, H.Y.; Data curation, Y.L.; Writing—original draft, H.Y. and S.L.; Writing—review & editing, H.Y. and S.L.; Supervision, H.Y.; Project administration, J.W. All authors have read and agreed to the published version of the manuscript.

Funding: National Natural Science Foundation of China (Grant No. 51975259).

Institutional Review Board Statement: Not applicable.

Informed Consent Statement: Not applicable.

Data Availability Statement: Not applicable.

Conflicts of Interest: The authors declare no conflict of interest.

References

1. Deng, Y. Study on the Technology of Osmanthus Glutinous Rice Candy Lotus Root Food. Master's Thesis, Nanjing Agricultural University, Nanjing, China, 2011.
2. Wang, M. Purification, Preliminary Structure Identification and Antioxidant Activity of Products Derived from Non-Enzymatic Browning in Lotus Root Filled with Sticky Rice and Control of Non-Enzymatic Browning. Master's Thesis, Nanjing Agricultural University, Nanjing, China, 2015.
3. Han, Y.; Gao, M.; Xiao, H.; Zhai, J.; Wang, Z.; Chen, X. Processing Technology and Irradiation Quality Guarantee of Waxy Rice Lotus Root. *Jiangsu Agric. Sci.* **2015**, *43*, 259–260.
4. Sun, J.; Chen, H.; Duan, J. Mechanical properties of the grooved-wheel drilling particles under multivariate interaction influenced based on 3D printing and EDEM simulation. *Comput. Electron. Agric.* **2020**, *172*, 105329. [[CrossRef](#)]

5. Cunha, R.N.; Santos, K.G.; Lima, R.N.; Duarte, C.R. Repose angle of monoparticles and binary mixture: An experimental and simulation study. *Powder Technol.* **2016**, *303*, 203–211. [[CrossRef](#)]
6. Ding, W.; Zhu, J.; Chen, W. Simulation calibration of highland barley contact parameters based on EDEM. *J. Chin. Agric. Mech.* **2021**, *9*, 114–121.
7. Han, D.; Zhang, D.; Yang, L. EDEM-CFD simulation and experiment of working performance of inside-filling air-blowing seed metering device in maize. *Trans. Chin. Soc. Agric. Eng.* **2017**, *13*, 23–31.
8. Cundall, P.A. A computer model for simulating progressive large-scale movements in blocky rock systems. *Proc. Int. Symp. Rock Mech.* **1971**, *1*, 11–18.
9. Cundall, P.A. The Measurement and Analysis of Acceleration on Rock Slopes. Ph.D. Thesis, Imperial College of Science and Technology, London, UK, 1971.
10. Stoimenov, N.; Ruzic, J. Analysis of the Particle Motion during Mechanical Alloying Using EDEM Software. *IFAC Pap. Online* **2019**, *52*, 462–466. [[CrossRef](#)]
11. Bobba, D.; Tabei, S.A.; Cherukuri, H.P.; Pando, M.A. DEM Simulation of Particle Segregation in Filling of Vibratory Dies. *Adv. Powder Technol.* **2020**, *31*, 3474–3484. [[CrossRef](#)]
12. Wang, G.; Hao, W.; Wang, J. *Discrete Element Method and Its Practice on EDEM*, 1st ed.; Northwest Polytechnical University Press: Xi'an, China, 2010.
13. Ye, F.; Liu, G.; Tang, L.; Jiang, X.; Li, C. Simulation of Canned Fruit Transportation Process Based on Discrete Element Method. *Package Eng.* **2021**, *4*, 189–196.
14. Li, F.; Yang, W.; Yang, J.; Mo, J. Simulation Model of Rice Electromagnetic Vibrated Seeding Based on DEM-MBD. *J. Agric. Mech. Res.* **2021**, *43*, 192–197.
15. Wu, C.; Wu, N.; Hu, C. Simulation of the Screw Conveyor Based on the DEM. *J. Chin. Agric. Mech.* **2015**, *36*, 92–94.
16. Sarangi, S.; Thalberg, K.; Frenning, G. Effect of Fine Particle Shape on the Stability and Performance of Adhesive Mixtures Intended for Inhalation. *Powder Technol.* **2021**, *385*, 299–305. [[CrossRef](#)]
17. Feng, X.; Liu, T.; Wang, L.; Yu, Y.; Zhang, S.; Song, L. Investigation on JKR Surface Energy of High-Humidity Maize Grains. *Powder Technol.* **2021**, *382*, 406–419. [[CrossRef](#)]
18. Santos, K.G.; Santana, R.C.; Souza, D.L.; Murata, V.V.; Barrozo, M.A.S. Spouting Behavior of Binary Particle Mixtures of Different Densities: Fluid Dynamics and Particle Segregation. *Particuology* **2019**, *42*, 58–66. [[CrossRef](#)]
19. Sebastian Escotet-Espinoza, M.; Foster, C.J.; Ierapetritou, M. Discrete Element Modeling (DEM) for Mixing of Cohesive Solids in Rotating Cylinders. *Powder Technol.* **2018**, *335*, 124–136. [[CrossRef](#)]
20. Yuan, Q.; Xu, L.; Xing, J. Parameter calibration of discrete element model of organic fertilizer particles for mechanical fertilization. *Trans. Chin. Soc. Agric. Eng.* **2018**, *34*, 21–27.
21. Liu, Y.; Zhang, T.; Liu, Y. Calibration and Experiment of Contact Parameters of Rice Grain Based on Discrete Element Method. *J. Agric. Sci Technol.* **2019**, *21*, 70–76.
22. Xiao, K.; Liu, T.; Xia, J.; Chen, Z. Biomechanics of lotus root. *J. Huazhong Agric. Univ.* **2016**, *35*, 125–130.
23. Yuan, Q.; Hu, L. Experimental Analysis on Influencing Factors of Cutting Resistance of Lotus Root. *Trans. Chin. Soc. Agric. Mach.* **2008**, *39*, 208–211.
24. Wu, T.; Huang, W.; Chen, X. Calibration of discrete element model parameters for cohesive soil considering the cohesion between particles. *J. South China Agric. Univ.* **2017**, *38*, 93–98.
25. Li, H.; Li, Y.; Tang, Z. Numerical simulation and analysis of vibration screening based on EDEM. *Trans. Chin. Soc. Agric. Eng.* **2011**, *27*, 117–121.
26. Pang, X. The Simulation of Material Movement in Whitening Chamber for A Sandy Roller Milling Machine. Master's Thesis, Henan University of Technology, Zhengzhou, China, 2015.
27. Zhou, J. Simulation and Experimental Research of Vertical Screw Conveyor Based on Discrete element Method. Master's Thesis, Zhejiang University of Technology, Hangzhou, China, 2018.
28. Li, Q. The Research of Granular Piling and Bulk Material Transfer Process Using DEM Simulation. Master's Thesis, Northeastern University, Shenyang, China, 2010.
29. Zhang, S.; Liu, Q.; Yang, P. Study on the Impurity Removal Device of Sugarcane Roller Based on Discrete Element Method. *Mod. Agric. Equip.* **2021**, *36*, 37–45.
30. Lu, J.; Zhang, J.; Li, W. Analysis on Influencing Factors of Granulated Particle Forming Based on Orthogonal Experiment Method. *J. North China Univ. Water Resour. Electr. Pow.* **2015**, *36*, 78–87.
31. Wang, C.; Liu, Y.; Zhang, Z.; Zhang, Z.H.; Han, L.; Li, Y.; Zhang, H.; Wongsuk, S.; Li, Y.; Wu, X. Spray performance evaluation of a six-rotor unmanned aerial vehicle sprayer for pesticide application using an orchard operation mode in apple orchards. *Pest Manag. Sci.* **2022**, *78*, 2449–2466. [[CrossRef](#)]
32. Wu, J.; Tang, Q.; Mu, S.; Jiang, L.; Hu, Z. Test and Optimization of Oilseed Rape (*Brassica napus* L.) Threshing Device Based on DEM. *Agriculture* **2022**, *12*, 1580. [[CrossRef](#)]
33. Li, Y.; Fan, J.; Hu, Z.; Luo, W.; Yang, H.; Shi, L.; Wu, F. Calibration of Discrete Element Model Parameters of Soil around Tubers during Potato Harvesting Period. *Agriculture* **2022**, *12*, 1475. [[CrossRef](#)]
34. Lie, X.; Gu, Z.; Wang, J. Waxy Rice Lotus Root Filling Machine. Chin. Patent 200910027708.5, 24 November 2010.

35. Yan, S.L.; Tu, Y.X.; Liu, J.H. Automatic Filling Device and Filling System of Glutinous Rice Root. Chin. Patent CN207767469U, 28 August 2018.
36. Zhang, H.; Hu, X.J.; Zhang, C.J. An Automatic Rice Filling Machine for Lotus Root. Chin. Patent CN109820221A, 31 May 2019.
37. Bai, H.Z. Semi-Automatic Filling Device for Waxy Rice Lotus Root. Chin. Patent CN108936774A, 7 December 2018.
38. Deng, Y.X.; Wan, J.S.; Wan, X.S. A Device for Filling Glutinous Rice with Lotus Root. Chin. Patent CN210248344U, 7 April 2020.
39. Xie, B.S.; Ma, L.X.; Gu, Q.L. A New Type of High Efficient Rice Filling Device for Glutinous Rice Root. Chin. Patent CN109090671A, 28 December 2018.